Pergamon
www.elsevier.com/locate/asr

Adv. Space Res. Vol. 27, Nos 6–7, pp. 1065–1069, 2001

Printed in Great Britain
0273-1177/01 $20.00 + 0.00
PII: S0273-1177(01)00139-9

INDO-GERMAN LOW-LATITUDE PROJECT DEOS: PLASMA BUBBLES IN THE POST SUNSET AND NIGHTTIME SECTOR

H.Thiemann[1,†], J.J.Sojka[2], J.J.Eccles[2], P.B. Rao[3], P.V.S.Rama Rao[4], R.Sridharan[5], G.S.Lakhina[6]

[1] *Arbeitsgruppe Weltraumphysik und –technologie, D-79098 Freiburg, Germany*
[2] *Space Environment Corporation, Logan, Utah 84321, USA*
[3] *National MST Radar Facility, Tirupati 517502 India*
[4] *Andhra University, Waltair 530003, India*
[5] *Space Plasma Laboratory, VSSC, Trivandrum 695022, India*
[6] *Indian Institute of Geomagnetism, Colaba, Mumbai 400005, India*

ABSTRACT

Two spread-F flights were performed under equinox conditions in April and September 1998 from the Indian low-latitude station SHAR. Both flights detected plasma bubbles confined to a narrow longitudinal extent. Plasma parameters are measured under two different conditions in the post-sunset ionosphere; when the F-layer is moving upward (19:21 IST launch) and when the F-layer is stationary (20:41 IST launch). Low altitude bubbles during upwelling of the F-region in the prereversal current enhancement phase are characterized by turbulent, non Maxwellian regions. Transitional scale waves with k=-3.6 are observed in the bubbles. This flight also detects strong sharp E-layers during downleg and an intermediate layer at 170km. Nighttime bubbles during almost stationary F-layer conditions show turbulent, Maxwellian features with moderate cooling compared to the undisturbed environment. Transitional scale waves in the bubble region show a spectral index k=-3.1. The spectral power is reduced by around 20dB compared to the sunset flight.

INTRODUCTION

Three RH 560 MK II rockets were launched from the Indian low-latitude station SHAR (13.7°N, 80.2°E) under equinox conditions in 1998 during the Indo-German rocket campaign DEOS (Dynamics of the Equatorial ionosphere Over SHAR). DEOS Rocket campaign is comparable to the Condor Rocket campaign of 1986 in Brazil (Kelley et al., 1986). DEOS campaign offers a different set of insitu and ground-based examination of the post-sunset physics of equatorial spread F in the India sector. Indian ionosonde and magnetometer network provided support observations and radio beacons were also carried aboard the rockets.

The rocket campaign DEOS and the scientific payload have been described by Thiemann et al. (1999). Since one flight had problems with nose cone ejection, we concentrate on two flights, launched on April 19, 1998 at 19:21 IST (flight F05) and September 28, 1998 at 20:41 IST (flight F06). Ionosonde measurements identified bottomside spread F, starting around 20:00 IST (Indian Standard Time) for both launch days. Range spreading was 200km and 130km for F05 and F06, respectively. The first flight was performed during the prereversal current enhancement phase.

We present data from two Langmuir probes. One spherical Langmuir probe is operated in a sawtooth swept voltage mode. Hysteresis effects have been studied with reasonable agreement of the plasma parameters in both voltage ranges. A critical parameter in the evaluation of Langmuir curves is a reliable derivation of the plasma potential Φ_{pp}. Pfaff (1996) identified Φ_{pp} as last point with the exponential rise in the current. Another approach (see e.g. Hirt et al., 1999) takes the inflection point between electron retardation and saturation region as defined by $I(\Phi_{pp})=0$. Both methods agree for ideal conditions with a sharp transition between retardation and saturation region. Normal collectors, however, show energy smearing of the electron retardation region due to work function patchiness (Brace, 1998) with associated smooth current transition. Therefore, we derive the plasma potential by the intersection of the extrapolated retardation and the saturation currents. The approximated retardation current follows by extrapolating linearly the largest slope m_{log} of the logarithmic current characteristic. Electron temperature is derived from the largest value of m_{log},

[†] In memoriam.

and electron density from the current at Φ_{pp}. To evaluate also small probe current data, a sliding average procedure of 10 Langmuir curves has been applied.

Fluctuations in a frequency range up to 3.1 kHz are measured by a second Langmuir probe. Designed as a high pass filter, this probe provides reliable measurements starting around 10Hz.

ELECTRON DENSITY AND TEMPERATURE

The ionospheric conditions are described by the motion of the F-layer as seen by ionosonde measurements over SHAR. Figure 1 shows the height of the bottomside F layer h'F versus local time (IST). The vertical bars mark the corresponding time of launch. The first rocket (flight F05) is launched at 19:21 IST while the F-layer moves upward, the other rocket (flight F06) at 20:41 IST when the F-layer is quite stationary.

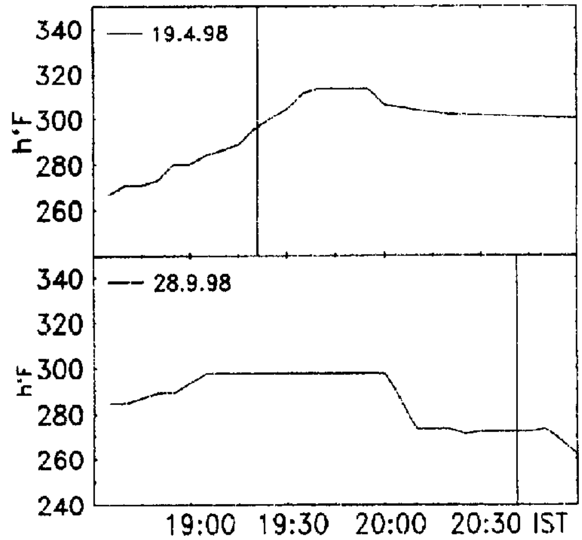

Fig. 1. Virtual height of F-layer versus local time. Vertical line gives time of launch.

Plasma parameters derived from the equinox flights in April and September 1998 are shown in Figure 2 and 3. For the different altitude regions, the solid and dotted lines characterize the quality of the instrumental resolution. In the low altitude region (dots) data points are derived from small probe currents with associated low density and instrumental accuracy in contrast to the higher altitude region (solid curves).

The F05 flight density profile shows undisturbed plasma conditions in the upleg phase. E-region features are completely missing. An intermediate layer appears to form around 180km. After a weak F-region valley around 240km, we note the transition to a pronounced F layer, where the F- maximum altitude is not reached yet. Significant structures are observed during downleg. Two sharp E-region layers at 100 and 118km extent vertically around 10 and 6km, respectively. They show around 20 times increased densities compared to the ambient background density. A deep E-region valley forms around 140km, followed by a clear intermediate layer at 170km and a F-region valley between 200 and 230km. Below the bottomside F-layer we observe two plasma bubbles at 257 and 270km in the density gradient region. The F-region maximum is reached at 410km.

Electron temperature measurements show comparable up- and downleg profiles in the F-region with temperatures increasing fom 1000 to 1500K between 300 and 430km. At lower altitudes we note a strong increase of electron temperature with decreasing densities. This effect is caused by the low currents and the

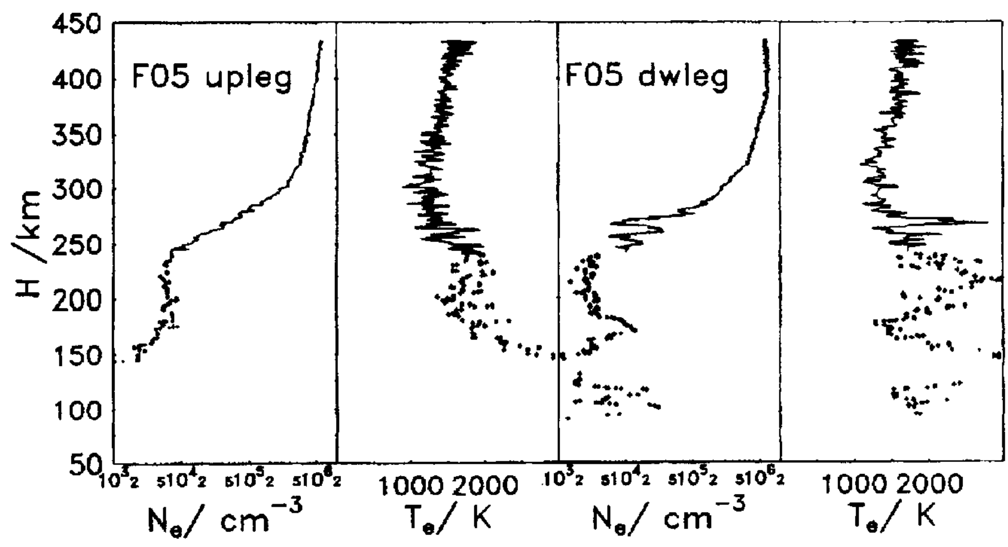

Fig. 2. Up- and downleg electron density and temperature profiles for flight F05 (19.4.1998, 19:21 IST).

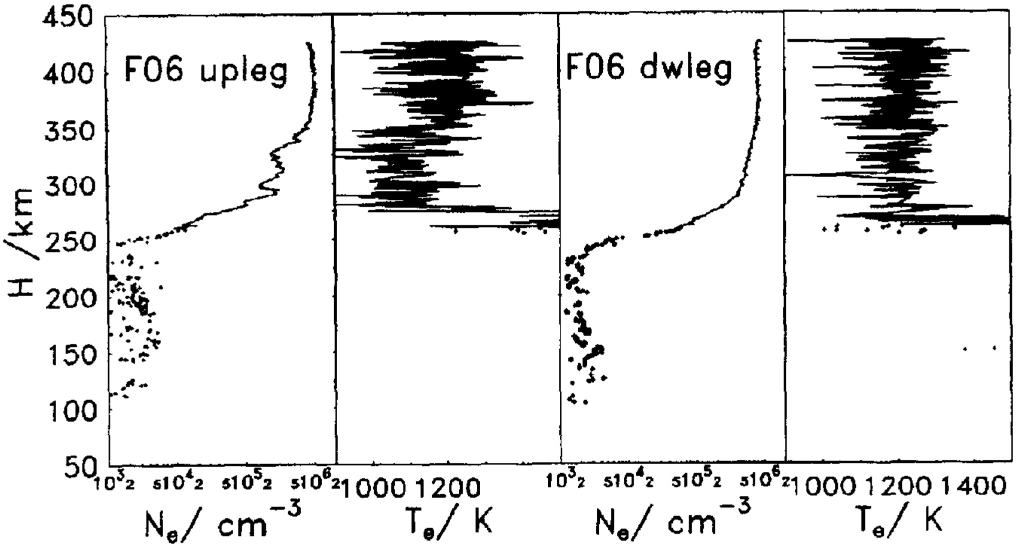

Fig. 3. Up- and downleg electron density and temperature profiles for flight F06 (28.9.1998, 20:41 IST)

large voltage increment of 95mV of the Langmuir probe, which tends to produce higher temperatures. With higher densities in the intermediate and the E-region layers of the downleg profile, the temperatures approach again the values of the F-region, suggesting almost constant temperatures around 1100K in the whole lower altitude range. Prominent features are the temperature peaks, which correlate with the density bubbles, and which are not related to the instrumental resolution.

Plasma parameters derived from the September 1998 flight are shown in Figure 3. The F-layers in both flight phases are very pronounced. Plasma bubbles are only observed during ascent in an altitude region between 290 and 350km. The F-region maximum is located at 390km (upleg) and 370km (downleg). Steep density gradients at the bottomside F region characterize the transition to the F-region valley. Structures at still lower altitudes are affected by the small probe currents, producing noisy density signatures. The upleg electron temperature profile shows values around 1100K in the bubble region and around 1200K in upper altitudes. For altitudes <250km, temperatures are unrealistically enhanced up to 2500K and more. We observe again the increase of temperature with drastically decreasing densities. The downleg profile shows temperatures around 1200K without significant variation in the relevant altitude region. The bubble region shows in contrast to the F05 flight reduced temperatures.

DISTRIBUTION FUNCTION

The second derivative of the current-voltage characteristic is related to the Maxwellian electron distribution function, where spherical Langmuir probes are also able to derive anisotropic distributions (Schott, 1968). With a probe surface A, the energy distribution function F(E) is given e.g. by Oyama and Hirao (1985).

$$F(E) = \frac{4 \cdot m_e^{1/2}}{\sqrt{2} \cdot A \cdot e^{3/2} \cdot N_e} \cdot \sqrt{E} \cdot \frac{d^2 I}{dE^2}$$

E= Φ_{pp}- U_P is the voltage equivalent of the particle energy with the probe potential U_P and the plasma potential Φ_{pp}. We use the corrected, extrapolated retardation current and the derived electron density. Significant altitude variation of the distribution function for the F05 flight is found in the bubble region during downleg, where the distribution functions show pronounced modifications of the Maxwellian features. Electrons are energized at the expense of low energy electrons. Selected distribution functions for 3 representative regions of the downleg bubbles are shown in Figure 4. Figure 4 left panel refers to the density depletion at 270km, Figure 4 right panel to the density depletion at 257km and Figure 4 center panel to the density maximum at 264km. The electrons are almost Maxwellian at the location of the density maximum. In the depleted regions, the electrons are not only heated, but show also significant deviations from the Maxwellian. The distribution functions in the bubble region are quite dynamic and have been averaged over around 2 km. Enhanced, and different temperatures in the upper and lower bubble shown in Figure 2 correlate with the thermal spread in the distribution function. Different features are seen in flight F06. The reduced temperatures observed in Figure 3 are related to Maxwellian distributions. The upleg- (bubble altitudes) and downleg- (undisturbed conditions) distribution functions at 300km are shown in Figure 5. The dots represent interpolated measurements and the dashed curve the associated Maxwellian distributions. The Maxwellian features of the measurements are evident. The distribution function finally provides a test for our data evaluation, since the integrated distribution function represents the electron density. Except for small densities $<10^{-4}cm^{-3}$, we found agreement within ±10%.

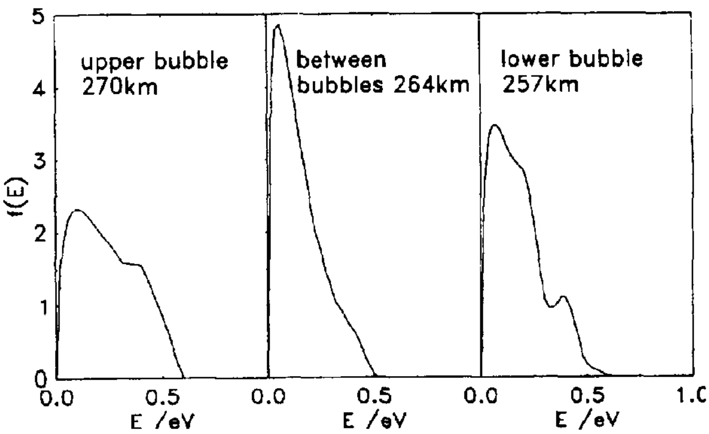

Fig. 4. Energy distribution function for selected altitude regions in plasma bubbles of flight F05.

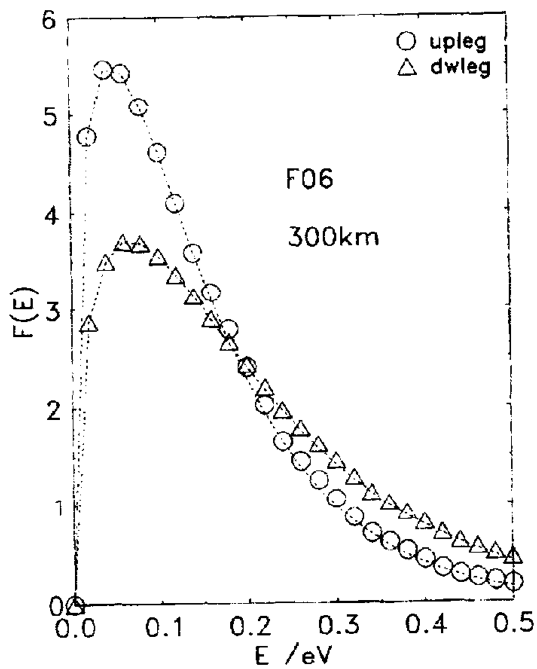

Fig. 5. Energy distribution function at 300km for flight F06.

SPECTRAL RESULTS

For spectral studies we use $(\partial I/I)^2$ derived from the fluctuation mode of the second Langmuir probe and the smoothed saturation current of the other probe. $(\partial I/I)^2$ is often used as indication of $(\partial n/n)^2$. Spectrograms versus altitude identify local turbulent regions defined by the bubble location in the flights F05 and F06. Ascent of F05 and descent of F06, where no bubbles are seen, show reduced power and no significant local spectral features.

Wavenumber spectra in- and outside the bubble region are shown in Figure 6. The spectra labeled 1 refer to inside the bubble region (255km for F05 and 317km for F06), those labeled 2 to outside the bubble region (300km for F05 and 382km for F06.) The wavenumber is defined by $k=1/\lambda$. The spectra are obtained for a typical altitude range of ±1km. For both flights we observe enhanced spectral power inside the bubble region. The spectral power in the bubble region of flight F05 simultaneously exceeds the level of the bubble region of F06 by around 20dB. Spectra with comparable power comparable to F06 results have been found during the PLUMEX I campaign (Kelley et al., 1982). Though the dynamic range of the irregularity amplitude is limited, we note pronounced transitional scale irregularities between around 5m and 40m. The spectral index in the F05 and F06 bubble is k=–3.6 and k=–3.2, respectively.

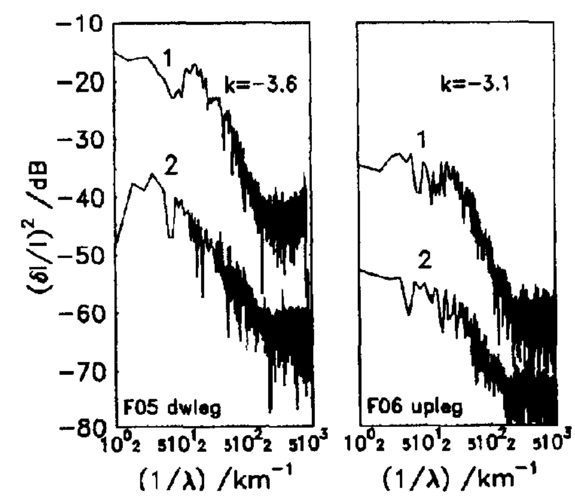

Fig. 6. Wavenumber spectra for F05 (left) and F06 (right). Spectra taken inside bubbles are labelled 1. Spectra outside bubbles are labelled 2.

SUMMARY

Sharp E-region layers similar to those of flight F05 were also detected by Raizada and Sinha (2000) during strong spread F. A comparison is given by Gupta and Thiemann (2000).

Intermediate layers have been observed the first time over SHAR. The two profiles of the post sunset flight suggest meridional neutral winds in the valley region between the E and F regions, where a tidal like meridional wind profile acts to deplete the background density and enhances the density in the intermediate layer (Ostermann et al., 1994).

Plasma bubbles in the two flights are detected either during descent or ascent, confirming qualitatively a case study of the evolution of equatorial plasma bubbles, which are confined to a narrow longitudinal extent as they drift eastward (Whalen, 2000).

Bubbles seen in the postsunset flight at low altitudes (240-270km) show temperature enhancements between 500 and 1000K compared to the undisturbed environment. The regions of high temperatures are associated with very high turbulence and a fluctuation level in the nonlinear range. The non Maxwellian distribution functions are assigned to the bubble regions and suggest nonlinear wave heating. Density depletion, wave activity and modification of the distribution function are clearly correlated.

Bubbles seen during the nighttime flight are detected in the bottomside F-layer at altitudes between 290 and 350km. The spectral power in the bubbles is reduced by about 20dB compared to the evening flight. Electron temperatures reduced by about 100K are related to the bubbles in the bottomside F-region. The distribution functions in- and outside the bubbles keep their Maxwellian characteristics. A cooling mechanism that accounts for the reduced bubble temperatures is still an open question.

ACKNOWLEDGMENTS

The work at AWT has been supported by the Bundesminister für Forschung und Technologie under grant 50 OE 9505 3. The authors gratefully acknowledge the support by Deutsches Zentrum für Luft- und Raumfahrt (DLR), Bonn and Indian Space Research Organization (ISRO), Bangalore. Authors are grateful to the staff of Vikram Sarabhai Space Center (VSSC), Trivandrum and Sriharikota rocket range (SHAR) for providing all the necessary facilities and support for this rocket flight.

REFERENCES

Brace, L.H., Langmuir probe measurements in the ionosphere, in *Measurement Techniques in Space Plasmas: Particles*, 23-35, AGU Geophysical Monograph 102, (1998).

Gupta, S.P. and H. Thiemann, Layers in the low latitude E-region over SHAR during evening and night hours, *Adv. Space Res.*, in press (2000).

Hirt, M., C.T. Steigies, A. Piel, and H. Thiemann, Langmuir probe diagnostics of the equatorial ionosphere: first results from DEOS flights F05/F06, Proceedings 14th ESA Symposium on European Rocket and Balloon Programmes and Related Research, Potsdam, Germany, ESA SP-437, 417-422, (1999).

Kelley, M.C., R. Pfaff, K.D. Baker, J.C. Ulwick, R. Livingston, C. Rino, and R. Tsunoda, Simultaneous rocket probe and radar measurements of equatorial spread F- transitional and short wavelength results, *J. Geophys. Res.*, **87**,1575 (1982).

Kelley, M.C., J. LaBelle, E. Kudeki, B.G. Fejer, S. Basu, Su. et al., The Condor equatorial spread F campaign: Overview and results of the large scale measurements, *J. Geophys. Res.*, **91**, 5487, 1986.

Pfaff, R.F., In-situ measurement techniques for ionospheric research, *Modern Ionospheric Science* (H. Kohl, R. Rüster, K. Schlegel eds.), European Geophysical Society, 459 (1996).

Osterman, G.B., R.A. Heelis and G.J. Bailey, Modeling the formation of intermediate layers at Arecibo latitudes, *J. Geophys. Res.*, **99**, 11357 (1994).

Oyama, K. and K. Hirao, Energy gain of supra-thermal electrons from the excited neutral gas, *J. Geomag. Geoelectr.*, **37**, 913 (1985).

Raizada, S. and H.S.S.Sinha, Some features of electron density irregularities over SHAR during strong spread F, *Ann. Geophysicae*, **18**, 141 (2000).

Schott, L., Electrical probes, in *Plasma Diagnostics* edited by W. Lochte-Holtgreven, North-Holland Publishing Company, Amsterdam, 668 (1968).

Thiemann, H., G. Mayer, A. Piel, C. Steigies, P.V.S. Rama Rao, P.B. Rao, R. Sridharan, and V.V. Somayajulu, DEOS: rocket investigations of the Indian low-latitude ionosphere, Proceedings 14th ESA Symposium on European Rocket and Balloon Programmes and Related Research, Potsdam, Germany, 31 May-3 June 1999, ESA SP-437 (September 1999).

Whalen, J.A., An equatorial bubble: its evolution observed in relation to bottomside spread F and to the Appleton anomaly, *J. Geophys. Res.*, **105**, 5303 (2000).